



1 **Validation of SOFIE nitric oxide measurements**

2 **Mark E. Hervig<sup>1,\*</sup>, Benjamin T. Marshall<sup>2</sup>, Scott M. Bailey<sup>3</sup>, David E. Siskind<sup>4</sup>, James M.**  
3 **Russell III<sup>5</sup>, Charles Bardeen<sup>6</sup>, Kaley A. Walker<sup>7</sup>, Bernd Funke<sup>8</sup>**

4 <sup>1</sup>GATS, Driggs, Idaho, USA.

5 <sup>2</sup>GATS, Hampton, Virginia, USA.

6 <sup>3</sup>Virginia Polytechnic Institute, Blacksburg, Virginia, USA.

7 <sup>4</sup>Space Science Division, Naval Research Laboratory, Washington, DC, USA.

8 <sup>5</sup>Hampton University, Hampton, Virginia, USA.

9 <sup>6</sup>NCAR, Boulder, Colorado, USA.

10 <sup>7</sup>Department of Physics, University of Toronto, Toronto, Canada.

11 <sup>8</sup>Instituto de Astrofísica de Andalucía, CSIC, Granada, Spain.

12 \*Corresponding author. E-mail address: [m.e.hervig@gats-inc.com](mailto:m.e.hervig@gats-inc.com) (M. Hervig).

13

14 **Abstract.** Nitric oxide (NO) measurements from the Solar Occultation for Ice Experiment  
15 (SOFIE) are validated through detailed uncertainty analysis and comparisons with independent  
16 observations. SOFIE was compared with coincident satellite measurements from the Atmospheric  
17 Chemistry Experiment (ACE) - Fourier Transform Spectrometer (FTS) instrument, and the  
18 Michelson Interferometer for Passive Atmospheric Sounding (MIPAS) instrument. The  
19 comparisons indicate mean differences of less than ~50% for altitudes from roughly 50 to 105 km  
20 for SOFIE spacecraft sunrise, and 50 to 140 km for SOFIE sunsets. Comparisons of NO time series  
21 show a high degree of correlation between SOFIE and both ACE and MIPAS for altitudes below  
22 ~130 km, indicating that measured NO variability in time is robust. SOFIE uncertainties increase  
23 below ~80 km due to interfering H<sub>2</sub>O absorption, and from signal correction uncertainties which



24 are larger for spacecraft sunrise compared to sunset. These errors are sufficiently large in sunrises  
25 that reliable NO measurements are infrequent below ~80 km.

## 26 **1. Introduction**

27 The Solar Occultation for Ice Experiment (SOFIE) has measured nitric oxide (NO) from  
28 the Aeronomy of Ice in the mesosphere (AIM) satellite since May 2007. SOFIE NO measurements  
29 have been the topic of numerous science investigations, including studies of thermosphere -  
30 stratosphere coupling (Bailey et al., 2015; Siskind et al., 2015; Hendrickx et al., 2018), effects of  
31 the 27-day solar rotation (Hendrickx et al., 2015), and the roles of dynamics and chemistry in  
32 diurnal variability (Siskind et al., 2019). SOFIE NO observations have also been used to determine  
33 the importance of changes in geomagnetic activity and solar radiation (Hendrickx et al., 2017),  
34 and to characterize the response of NO to electron precipitation (Smith-Johnsen et al., 2017; 2018;  
35 Newnham et al., 2018). SOFIE version 1.3 (V1.3) NO measurements are validated here through  
36 uncertainty analysis and comparisons with correlative measurements.

37 Coincident satellite measurements are from the Atmospheric Chemistry Experiment (ACE)  
38 - Fourier Transform Spectrometer (FTS) instrument, and the Michelson Interferometer for Passive  
39 Atmospheric Sounding (MIPAS) instrument. The ACE-FTS instrument has used solar occultation  
40 to measure more than 30 trace gases and over 20 isotopologues from 2004 to present (Bernath et  
41 al., 2005). ACE NO measurements span ~6 to 107 km altitude with a vertical resolution of ~3.5  
42 km, and retrievals are reported at the oversampled vertical interval of 1 km. This work used version  
43 3.5 NO retrievals, which are based on measurements between 5.056 and 6.063  $\mu\text{m}$  wavelength  
44 sampled with 39 micro-windows (Kerzenmacher et al., 2008; Sheese et al., 2016). The main  
45 interfering species in this region is  $\text{O}_3$ , with smaller contributions from  $\text{CO}_2$ ,  $\text{H}_2\text{O}$ , and  $\text{COF}_2$ .  
46 MIPAS operated onboard the Envisat satellite during 2005 – 2012 in a sun-synchronous orbit with



47 equator crossing at 10 am and 10 pm local time. MIPAS measured limb emission spectra covering  
48 4.15 to 14.6  $\mu\text{m}$  wavelength using a Fourier transform spectrometer. MIPAS primarily observed  
49 altitudes from 6 to 68 km, with periodic (one day in ten) observations extending into the  
50 thermosphere ( $\sim 150$  km). The MIPAS NO product is reported at 1 km intervals, but has a vertical  
51 resolution of 5 - 15 km, except within the upper mesosphere outside polar winter where the  
52 resolution degrades up to 20 km. NO emission measured at 5.3  $\mu\text{m}$  was used to retrieve NO volume  
53 mixing ratios (VMR) (Funke et al., 2005, Bermejo-Pantalón et al., 2011). The mixing ratios were  
54 converted to number densities (ND, molecules  $\text{cm}^{-3}$ ) using temperatures derived from 15  $\mu\text{m}$   
55 emissions below 100 km and from 5.3  $\mu\text{m}$  above (jointly retrieved with NO). This work uses data  
56 version V5r\_NOwT\_622. Bender et al (2015) report NO measurements comparisons including  
57 ACE, MIPAS, the SCanning Imaging Absorption spectroMeter for Atmospheric CHartographyY  
58 (SCIAMACHY) instrument, and the sub-millimeter radiometer (SMR) satellite instrument. They  
59 found mean differences of 30 to 100%, depending on latitude, season, and altitude.

## 60 **2. SOFIE Observations**

61 SOFIE uses solar occultation to measure vertical profiles of temperature, five gaseous  
62 species ( $\text{O}_3$ ,  $\text{H}_2\text{O}$ ,  $\text{CO}_2$ ,  $\text{CH}_4$ , and NO), polar mesospheric clouds (PMC), and meteoric smoke  
63 (Gordley et al., 2009; Hervig et al., 2009). NO measurements are accomplished using broadband  
64 ( $\sim 2\%$  filter width) measurements centered at 5.32  $\mu\text{m}$  wavelength. Gomez-Ramirez et al. (2013)  
65 describe the SOFIE NO observations, signal corrections, and retrievals. The photo conductive  
66 detector experiences a response oscillation due to the thermal shock of transitioning the field-of-  
67 view (FOV) from dark space to the sun, at the start of each observation. This thermal response  
68 artifact was successfully corrected in ground processing, resulting in NO retrievals that span  $\sim 30$   
69 to 149 km altitude. The SOFIE FOV subtends  $\sim 1.5$  km vertically, but retrieved NO has a coarser



70 effective vertical resolution (~2.5 km) due to measurement noise and retrieval errors. Gomez-  
71 Ramirez et al. compared SOFIE version 1.2 NO profiles to coincident ACE measurements for  
72 altitudes from 87 - 105 km, showing negligible differences for Southern Hemisphere (SH) SOFIE  
73 measurements (spacecraft sunset) and ~18% differences in the Northern Hemisphere (NH)  
74 (sunrise). SOFIE NO results are reported as both VMR and ND. SOFIE retrieves temperatures (T)  
75 from 17 - 100 km altitude, and T from the mass spectrometer incoherent scatter (MSIS) model are  
76 used above 100 km (see Marshall et al., 2011). Because VMR requires knowledge of air density  
77 (and thus T), the SOFIE VMR likely contain large errors above 100 km due to MSIS T  
78 uncertainties. NO ND has the advantage of being independent of T, and thus is recommended for  
79 use above 100 km.

80 SOFIE NO profiles contain values that indicate missing data (-1e24), which imply that the  
81 signal was either not measured or contained artifacts that rendered it unusable. There are also  
82 values which indicate a good measurement, but an unsuccessful retrieval ( $10^{-14}$  in VMR). These  
83 instances correspond to cases where the simulated signal considering interfering gases was greater  
84 than the observed signal. These situations clearly indicate errors in the interference, and/or the  
85 measured signals. In V1.3, the unsuccessful retrievals were included in vertical smoothing of the  
86 NO VMR profile prior to output, which resulted in large errors in the two points above and below  
87 the unsuccessful layer. These values were removed in post-processing, along with points  
88 associated with PMCs, which have erroneously increased NO (see details below). PMCs are  
89 clearly identified in SOFIE profiles using multi-wavelength observations as described in Hervig  
90 et al. (2009). The filtered profiles were then smoothed by box-car averaging on a 3 km vertical  
91 grid (see Figure 1a). The filtered and smoothed V1.3 NO profiles are available on the SOFIE  
92 webpage ([sofie.gats-inc.com](http://sofie.gats-inc.com)).



93 Figure 1b shows the fraction of successful SOFIE NO measurements as a function of  
94 altitude for SOFIE spacecraft sunrise and sunset. Between ~45 and 80 km, sunrises are successful  
95 less than 20% of the time, while sunsets are successful more than 50% of the time. This is  
96 comparable to ACE, which has a similar fraction of retrieval success at these heights, although no  
97 appreciable difference between spacecraft sunrise and sunset (Figure 1b). MIPAS has very few  
98 unsuccessful NO retrievals (<3%), and only reports the valid results. The often low fraction of  
99 good NO results below ~80 km should be born mind when using the SOFIE (and ACE) NO  
100 products.

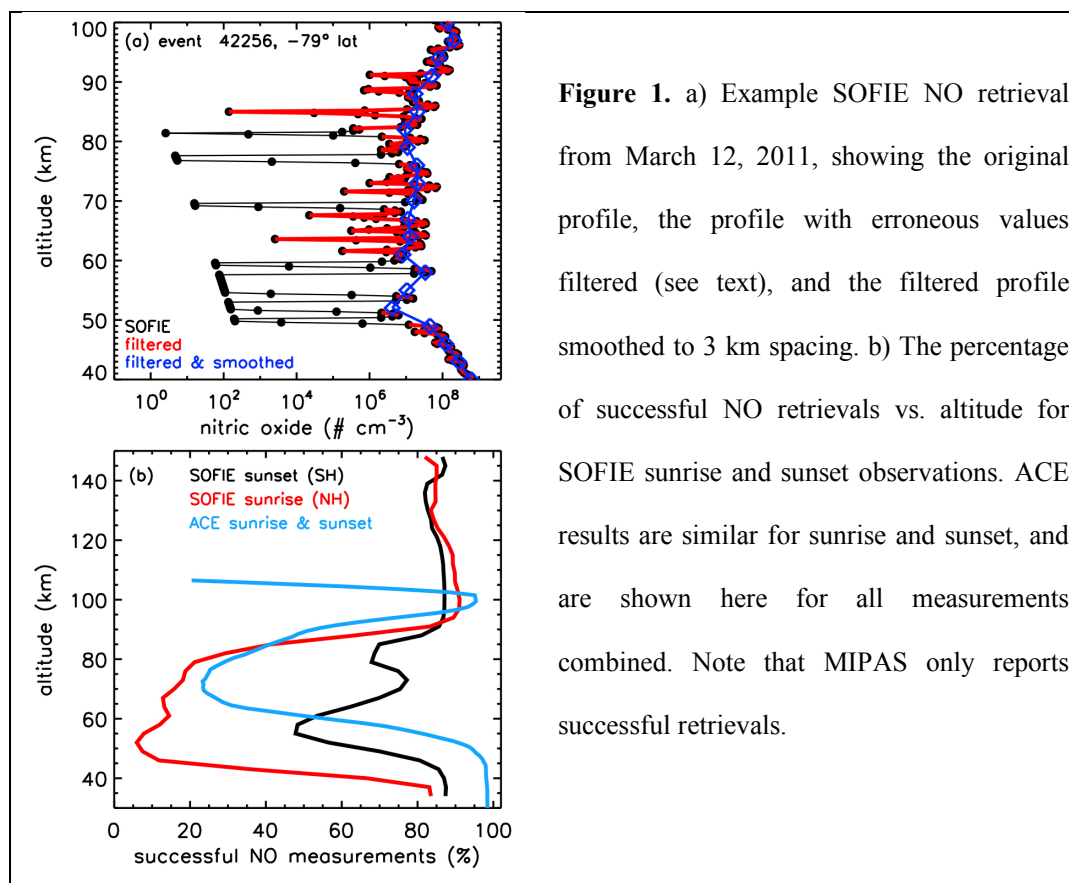


**Figure 1.** a) Example SOFIE NO retrieval from March 12, 2011, showing the original profile, the profile with erroneous values filtered (see text), and the filtered profile smoothed to 3 km spacing. b) The percentage of successful NO retrievals vs. altitude for SOFIE sunrise and sunset observations. ACE results are similar for sunrise and sunset, and are shown here for all measurements combined. Note that MIPAS only reports successful retrievals.



## 101 **2.1. Uncertainty Analysis**

102 The SOFIE NO uncertainty analysis presented here is an extension of the analysis  
103 described in Gomez-Ramirez et al. (2013). Retrieved NO ND error mechanisms can be categorized  
104 as due either to the SOFIE measurements, or to the signal simulations used in the retrievals.  
105 Simulation uncertainties include modeling errors, the representation of instrument characteristics  
106 (e.g., relative spectral response (RSR)), and the description of interfering gases and aerosols.

107 It is useful to first understand the relative signal contributions from interfering gases and  
108 aerosols in the SOFIE NO bandpass, as these can be the largest error sources. Figure 2 shows  
109 calculated signals considering polar summer conditions. The signal is due entirely to NO above  
110 ~85 km, with the main interference at lower altitudes coming from H<sub>2</sub>O, CO<sub>2</sub>, and O<sub>3</sub>. H<sub>2</sub>O  
111 interference is removed using SOFIE H<sub>2</sub>O measurements which cover ~20 to 95 km altitude and  
112 have uncertainties of ~15% (Rong et al., 2010). CO<sub>2</sub> is described using model results (Garcia et  
113 al., 2007) which have uncertainties of <5%. O<sub>3</sub> interference is removed using SOFIE O<sub>3</sub> retrievals  
114 that span ~55 - 110 km with uncertainties of <10% (Smith et al., 2013). Climatological O<sub>3</sub> is used  
115 below 55 km, which can have large uncertainties. Fortunately the O<sub>3</sub> contribution to the SOFIE  
116 NO signal is small at these heights (Figure 2). The upcoming SOFIE version (V1.4) will use new  
117 SOFIE O<sub>3</sub> retrievals that extend down to ~15 km altitude. Interference from stratospheric sulfate  
118 aerosols (SSA) is negligible above ~30 km, where NO is retrieved.

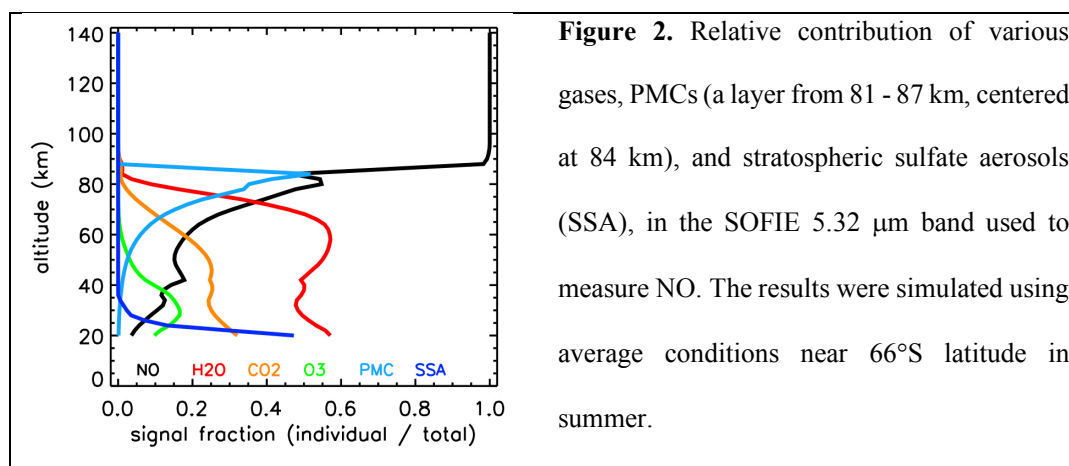
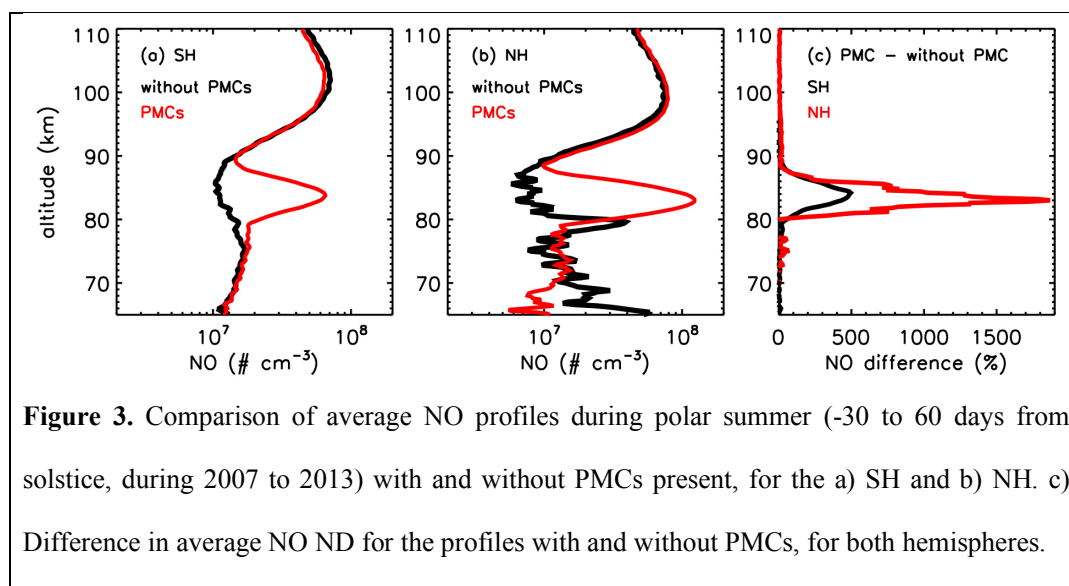


**Figure 2.** Relative contribution of various gases, PMCs (a layer from 81 - 87 km, centered at 84 km), and stratospheric sulfate aerosols (SSA), in the SOFIE 5.32  $\mu\text{m}$  band used to measure NO. The results were simulated using average conditions near 66°S latitude in summer.

119

120 PMCs, which appear during polar summer, can contribute a large fraction of the total  
121 SOFIE NO signal at PMC heights (~80 - 90 km). The example in Figure 2 is for a moderate PMC,  
122 which contributes ~50% of the total signal near 84 km. This example also illustrates that the PMC  
123 signal can extend from 20 to 30 km below the PMC layer, because the tangent path view includes  
124 a contribution from altitudes above. PMC interference is not removed in V1.3 (it will be in V1.4).  
125 The artificial increase in retrieved NO ND when PMCs are present is illustrated by comparing  
126 concurrent profiles with and without PMCs present, where the contamination is obvious at ~80 to  
127 90 km (Figures 3a and 3b). NO ND can be erroneously increased by factors of 10 or more by PMC  
128 contamination (Figure 3c), and it is thus imperative to not use NO when PMCs are present. Note  
129 that this effect is typically worse in the NH where PMCs typically have greater volume density  
130 (e.g., Hervig et al., 2009). Because the portion of NO profiles contaminated by PMCs has been  
131 removed in the SOFIE data file described above, it is recommended to either use those results, or  
132 ensure that PMC profiles are screened using the reported SOFIE PMC observations (Hervig et al.,  
133 2009). Because PMC-induced errors occur only during polar summer and not necessarily in every  
134 profile, PMC induced NO errors are not included in the total uncertainty estimates below.



135

136 The main error sources in retrieved NO are summarized in Table 1 for a range of altitudes.

137 The largest measurement errors are due to noise and the thermal response correction, which is

138 larger for sunrise observations than in sunsets (see Gomez-Ramirez et al. (2013) for details). The

139 remaining errors are in the category of measurement interpretation as encompassed by model

140 simulations of the SOFIE signal. Errors in the interfering gases (measured or modeled) were taken

141 from the relevant publications, as discussed above. Each error mechanism was imposed in the V1.3

142 SOFIE retrieval algorithm to determine the uncertainty induced in retrieved NO ND. The V1.3

143 SOFIE forward model uses HITRAN 2004 line parameters, which are estimated to have ~7%

144 systematic uncertainties for NO near 5.32  $\mu\text{m}$ . Altitude registration errors are estimated to be ~100

145 m (Marshall et al., 2011). While errors in temperature propagate directly into NO VMR, they do

146 not affect ND, which is a strong argument for using ND in the thermosphere where SOFIE does

147 not measure temperatures. The uncertainties in retrieved NO are summarized at key altitudes in

148 Table 1 for each mechanism, along with the total uncertainty. The largest four error sources are

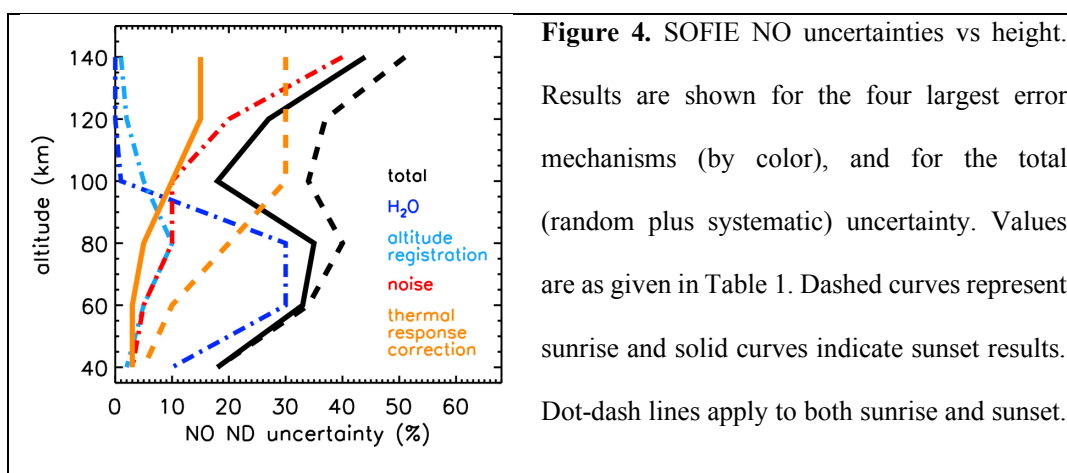


149 shown versus height in Figure 4, where it is clear that water vapor interference errors dominate  
 150 below ~90 km, for both sunrise and sunset. For sunset measurements NO ND errors are dominated  
 151 by noise above ~100 km. Sunrise NO errors are dominated by the thermal response correction  
 152 above ~90 km, as discussed by Gomez-Ramirez et al. (2013).

**Table 1.** Uncertainty (%) in retrieved NO number density versus altitude due to various random (R) and systematic (S) error mechanisms. Two values are listed when they were different for sunrise / sunset.

Error Source	Altitude (km)					
	140	120	100	80	60	40
Altitude Registration (S)	1	2	5	10	5	2
H <sub>2</sub> O Interference (S)	0	0	1	30	30	10
CO <sub>2</sub> Interference (S)	0	0	1	3	5	3
O <sub>3</sub> Interference (S)	0	0	0	1	3	10
Line Strengths (S)	7	7	7	7	7	7
Relative Spectral Response (S)	5	5	5	5	5	5
Field-of-View (S)	2	3	4	4	3	3
Forward Model (S)	3	3	3	3	3	3
Signal Noise (R)	40	20	10	10	5	3
Thermal Response Correction (R)	30 / 15	30 / 15	30 / 10	20 / 5	10 / 3	5 / 3
<b>Total (root sum squared)</b>	<b>51 / 44</b>	<b>37 / 27</b>	<b>34 / 18</b>	<b>40 / 35</b>	<b>34 / 33</b>	<b>18 / 18</b>

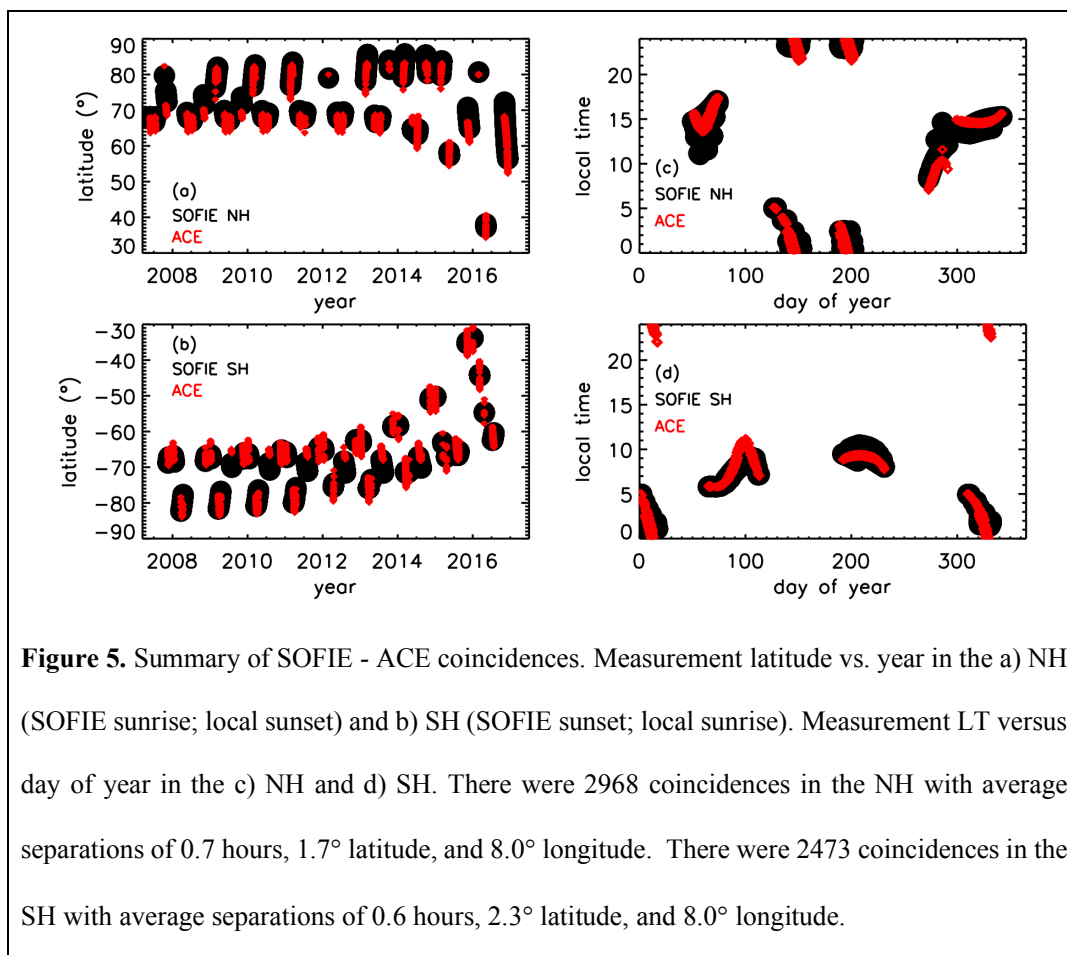
153





#### 154 **4. Measurement Comparisons**

155 Time separation is important in the measurement comparisons because NO abundance can  
156 have a strong diurnal dependence, with more than 10% per hour changes in ND near local sunrise  
157 or sunset, depending on altitude, latitude, and season (e.g., Siskind et al., 2019). This effect can be  
158 managed in the comparisons by 1) keeping the measurement separations as small as possible, or  
159 2) applying a modeled diurnal correction to measurements that are separated in time. Removing  
160 diurnal dependence using a model description was determined to induce unacceptably large  
161 uncertainties, in part because the model results are dependent on transport as well as  
162 photochemistry. The first approach was therefore adopted here, finding coincident measurement  
163 pairs for maximum separations of 2 hours UT, 4° latitude, and 20° longitude. Note that 20°  
164 longitude corresponds to ~1.3 hours in local time. These coincidence criteria insured that average  
165 measurement separations were less than one hour. Note that when this work mentions sunrise or  
166 sunset (for SOFIE and/or ACE) that it always refers to the view from orbit. SOFIE spacecraft  
167 sunset is always Earth sunrise (and vice versa), due to the retrograde polar orbit. ACE can have  
168 varying correspondence between sunset or sunrise as viewed from orbit or Earth, and thus it is  
169 important to track LT in the comparisons. Finally, the comparisons shown below include SOFIE  
170 profiles with PMCs, and the results do not change when excluding profiles with PMCs. This is  
171 because SOFIE NO results used here have been filtered at PMC heights when PMCs were present  
172 (see Section 2), and because the MIPAS and ACE NO measurements are not affected by PMC  
173 contamination (Funke et al., 2005; Kerzenmacher et al., 2008). SOFIE - ACE coincidences are  
174 illustrated in Figure 5 including a summary of the coincidence statistics, and SOFIE - MIPAS  
175 coincidences are shown in Figure 6.



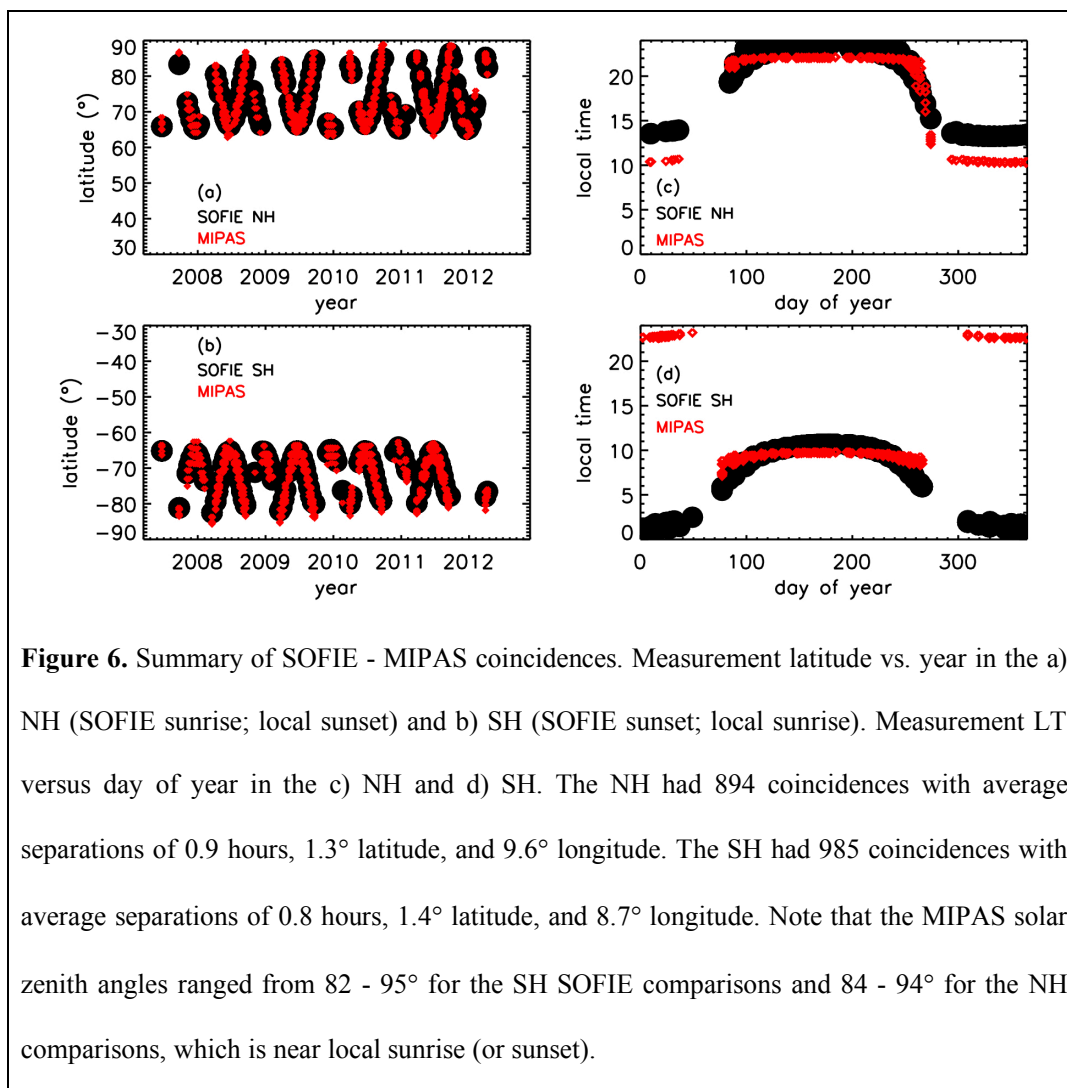


**Figure 6.** Summary of SOFIE - MIPAS coincidences. Measurement latitude vs. year in the a) NH (SOFIE sunrise; local sunset) and b) SH (SOFIE sunset; local sunrise). Measurement LT versus day of year in the c) NH and d) SH. The NH had 894 coincidences with average separations of 0.9 hours, 1.3° latitude, and 9.6° longitude. The SH had 985 coincidences with average separations of 0.8 hours, 1.4° latitude, and 8.7° longitude. Note that the MIPAS solar zenith angles ranged from 82 - 95° for the SH SOFIE comparisons and 84 - 94° for the NH comparisons, which is near local sunrise (or sunset).

177

178           SOFIE, ACE, and MIPAS have effective vertical resolution of roughly 2.5, 3.5, and >5km,  
179 respectively, despite differences in the FOVs and reported vertical spacing. For the comparisons  
180 shown here, the ACE and MIPAS results were interpolated to the SOFIE 3 km vertical scale, with  
181 no additional smoothing applied. Note that the results below are essentially unchanged if the NO  
182 profiles are interpolated to either the ACE or MIPAS vertical scales instead. Comparison of NO

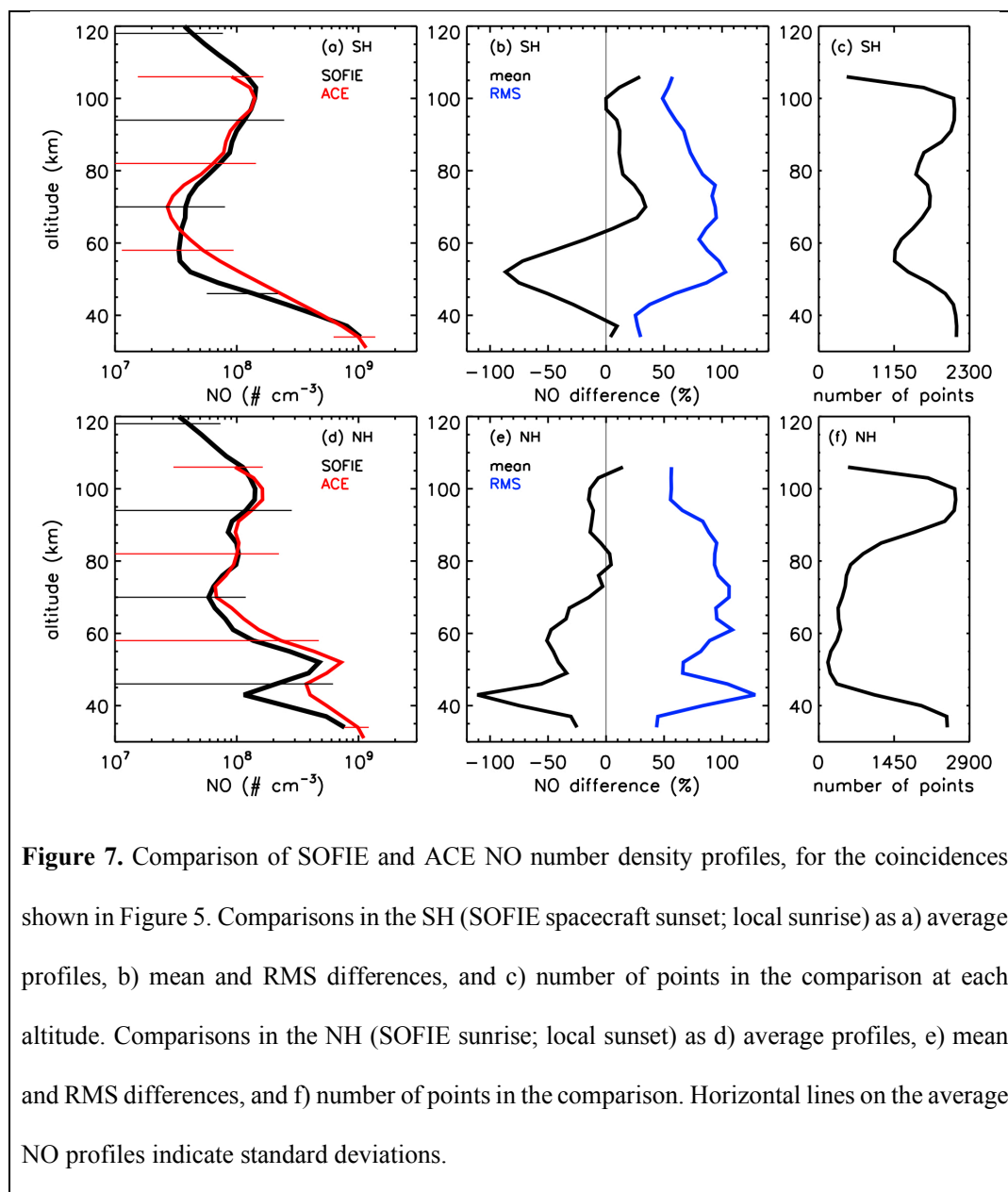


183 vertical profiles are shown in Figure 7 for SOFIE vs. ACE, and in Figure 8 for SOFIE vs. MIPAS.  
184 The comparisons are shown as average profiles, mean and root-mean-square (RMS; i.e. random  
185 plus systematic) differences, and the number of points used in the comparison at each altitude.  
186 SOFIE - ACE mean differences are within 50% for altitudes from ~50 to 107 km in both the SH  
187 and NH (Figures 7b and 7d). SOFIE - MIPAS differences are within ~50% for ~55 - 140 km in  
188 the SH (Figure 8). The NH MIPAS comparison indicates larger differences than in the SH, but  
189 with some similarities in the dependence on height (e.g. SOFIE > MIPAS near 140 km). The  
190 SOFIE - MIPAS comparison above ~130 km in the SH (~140 km in the NH) indicates an  
191 increasing bias with SOFIE suggesting higher NO. Siskind et al. (2019) noted a similar bias from  
192 indirect comparisons of SOFIE with the Student Nitric Oxide Explorer (SNOE) results. Note that  
193 the number of measurement pairs used in the comparisons is fairly consistent in height for the SH  
194 (SOFIE sunset), in both the ACE and MIPAS comparisons (Figures 7c and 8c). The NH (SOFIE  
195 sunrise) comparisons, however, have very few valid measurements between ~50 and 80 km  
196 (Figures 7f and 8f), due to the lack of good SOFIE (and sometimes ACE) results at these altitude  
197 for sunrise.

198 Comparing the SOFIE - ACE and SOFIE - MIPAS mean differences shows notable  
199 similarities in both the height dependence and magnitude of the differences, especially in the SH  
200 (Figure 9a). In particular, SOFIE NO is consistently ~50% or more lower than ACE and MIPAS  
201 near the stratopause (~50 km) in both the SH and NH (Figure 9). These similarities suggest the  
202 presence of a systematic error in SOFIE, although a potential error mechanism has not yet been  
203 identified. It should be noted that diurnal variations in NO, which are strongest in the stratosphere  
204 and thermosphere, can determine that occultation measurements are viewing through strong spatial  
205 gradients along the tangent path. The impact of such gradients has not yet been quantified, but

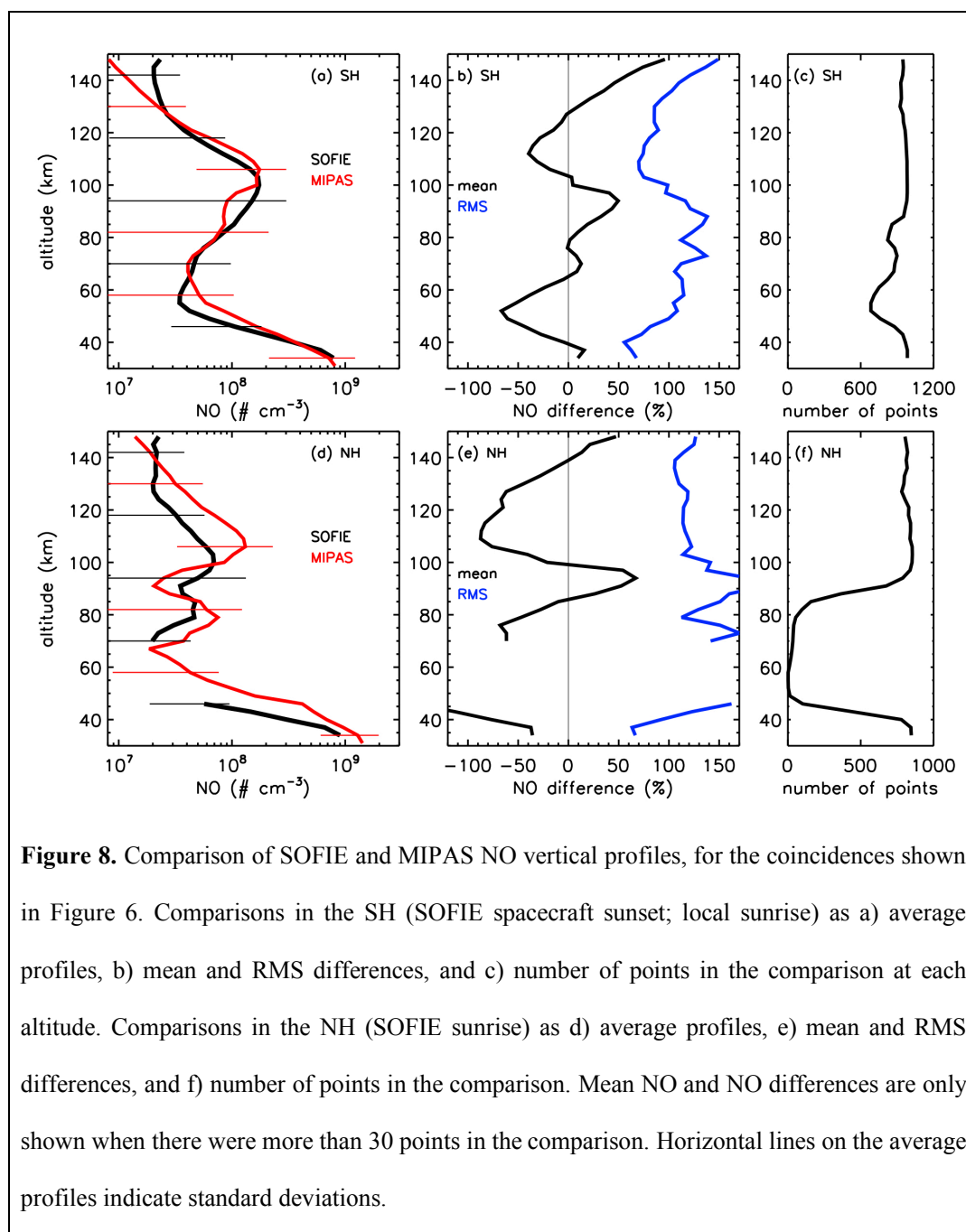


206 should appear as a systematic bias in retrieved NO. Note that the comparisons in the NH  
207 additionally indicate that MIPAS NO is greater than ACE, particularly below ~90 km (Figure 9b),  
208 a difference that was also reported by Bender et al. (2015).



**Figure 7.** Comparison of SOFIE and ACE NO number density profiles, for the coincidences shown in Figure 5. Comparisons in the SH (SOFIE spacecraft sunset; local sunrise) as a) average profiles, b) mean and RMS differences, and c) number of points in the comparison at each altitude. Comparisons in the NH (SOFIE sunrise; local sunset) as d) average profiles, e) mean and RMS differences, and f) number of points in the comparison. Horizontal lines on the average NO profiles indicate standard deviations.

209



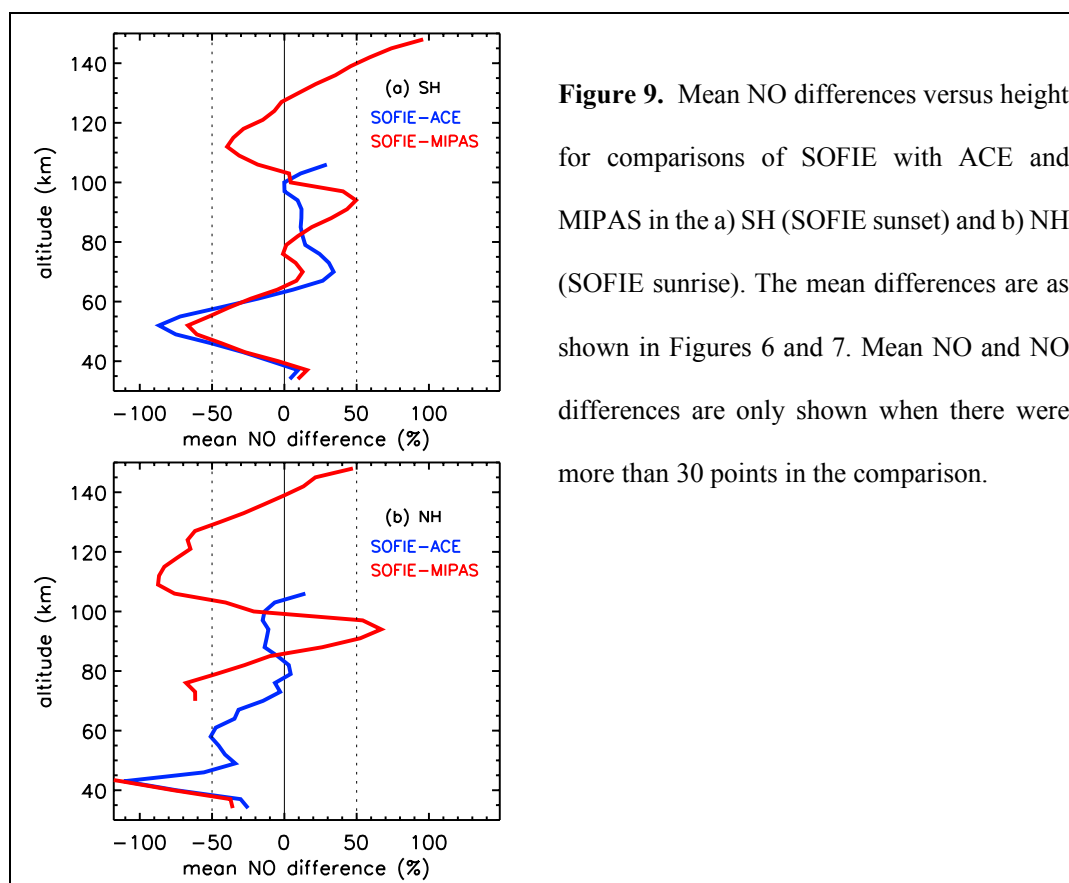


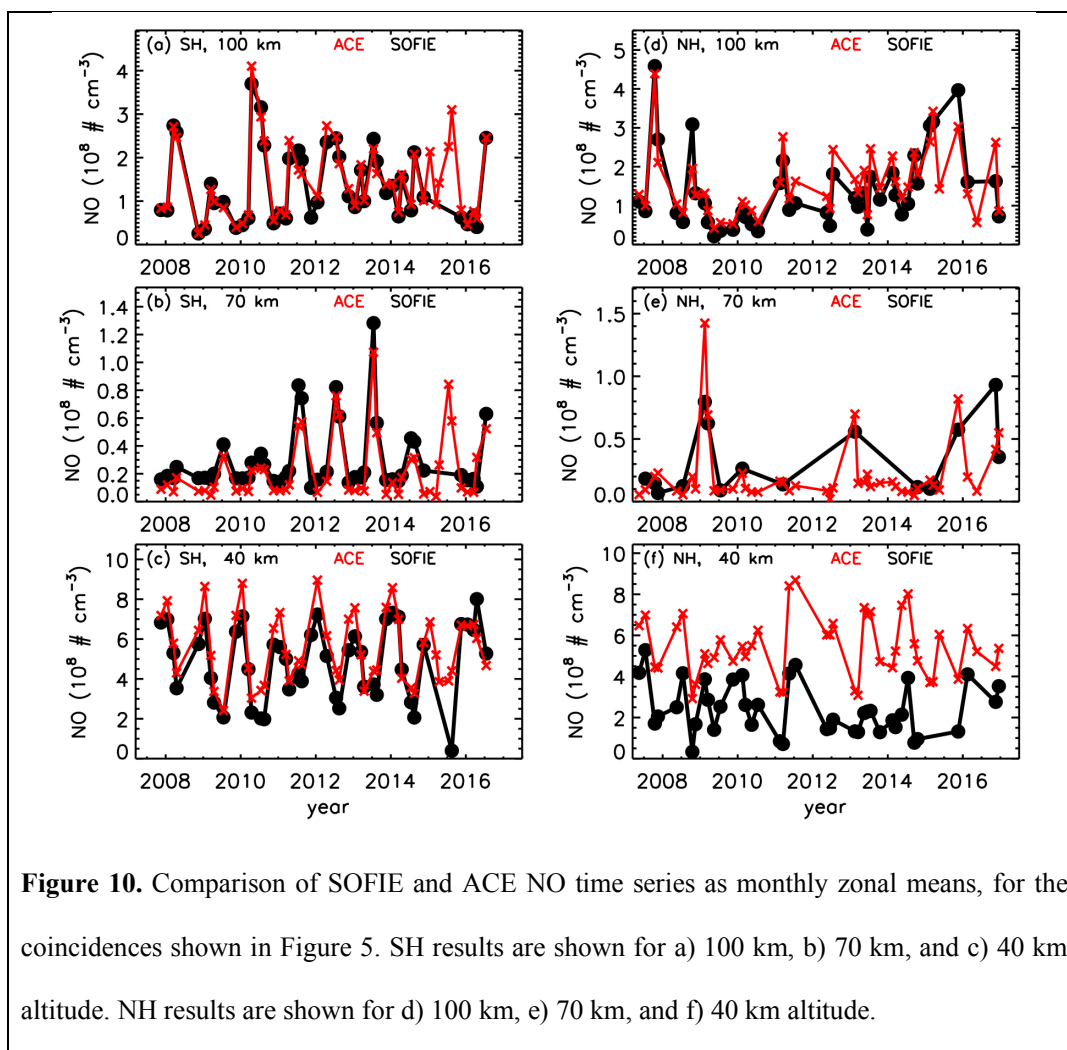
**Figure 9.** Mean NO differences versus height for comparisons of SOFIE with ACE and MIPAS in the a) SH (SOFIE sunset) and b) NH (SOFIE sunrise). The mean differences are as shown in Figures 6 and 7. Mean NO and NO differences are only shown when there were more than 30 points in the comparison.

211

212 Time series of monthly zonal mean NO at selected altitudes are compared for the SOFIE -  
213 ACE coincidences in Figure 10, and for the SOFIE - MIPAS coincidences in Figure 11. These  
214 time series indicate good agreement on the timing and magnitude of NO variations, despite  
215 systematic differences at certain altitudes. To better quantify the agreement concerning time  
216 variations, linear correlation coefficients were determined for each height in the SOFIE - ACE and  
217 SOFIE - MIPAS comparisons. Results in the SH (Figure 12a) show a strong correlation between  
218 SOFIE and ACE or MIPAS for altitudes below ~130 km. Results in the NH (Figure 12b) indicate  
219 a significant correlation between SOFIE and ACE for 90 - 107 km. The NH SOFIE - MIPAS  
220 comparisons also indicate a high correlation for ~90 - 110 km. Note that the correlations were not



221 determine in the NH for ~50 to 85 km because there were very few SOFIE NO retrievals (e.g.  
222 Figures 10e and 11g).



223

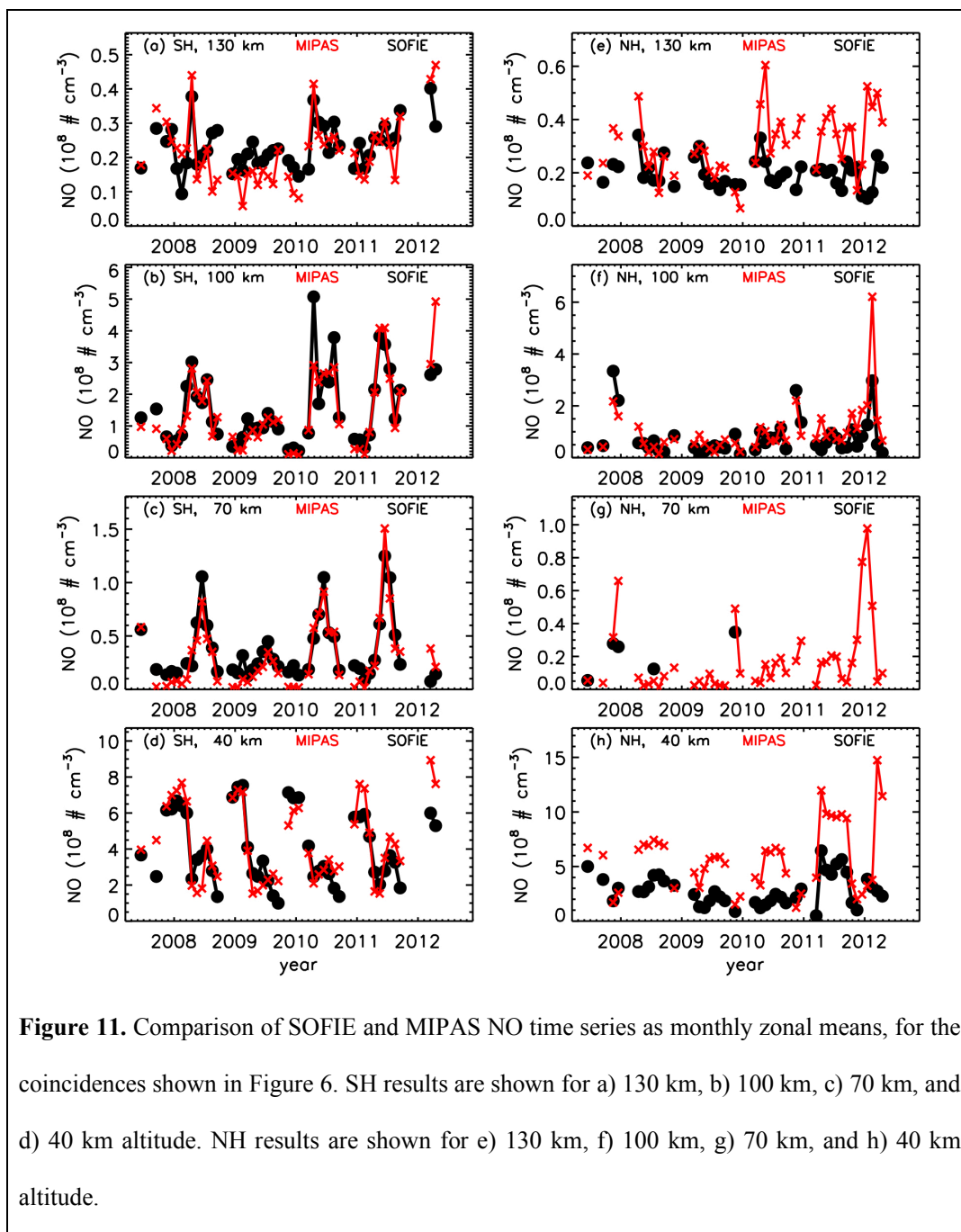


**Figure 11.** Comparison of SOFIE and MIPAS NO time series as monthly zonal means, for the coincidences shown in Figure 6. SH results are shown for a) 130 km, b) 100 km, c) 70 km, and d) 40 km altitude. NH results are shown for e) 130 km, f) 100 km, g) 70 km, and h) 40 km altitude.

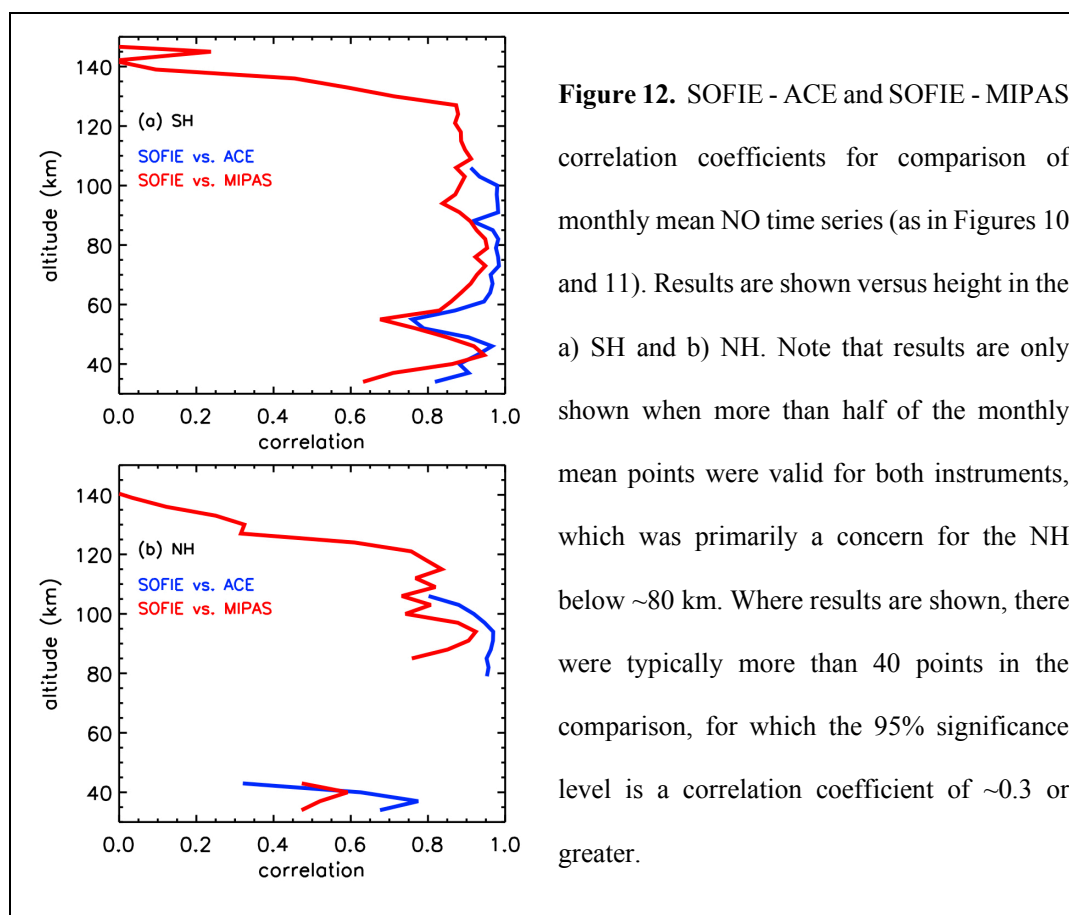


**Figure 12.** SOFIE - ACE and SOFIE - MIPAS correlation coefficients for comparison of monthly mean NO time series (as in Figures 10 and 11). Results are shown versus height in the a) SH and b) NH. Note that results are only shown when more than half of the monthly mean points were valid for both instruments, which was primarily a concern for the NH below ~80 km. Where results are shown, there were typically more than 40 points in the comparison, for which the 95% significance level is a correlation coefficient of ~0.3 or greater.

## 225 5. Summary

226 Comparisons of SOFIE NO with coincident measurements from ACE and MIPAS indicate  
227 mean differences of less than ~50% for altitudes from roughly 50 to 105 km for SOFIE spacecraft  
228 sunrise, and ~50 to 140 km for SOFIE sunsets. Comparisons of NO time series show significant  
229 correlation between SOFIE and either ACE or MIPAS for altitudes of ~40 - 130 km in the SH,  
230 indicating that measured NO variability is robust. Correlations were significant in the NH for ~90  
231 to 130 km, but not at lower heights due to the sparse SOFIE results in that altitude range. SOFIE  
232 uncertainties increase below ~85 km due primarily to interfering H<sub>2</sub>O absorption and signal



233 correction errors. These effects are sufficiently large in SOFIE sunrise measurements that retrieved  
234 NO is only reliable below ~80 km during enhancement events (in <20% of the data), such as  
235 downward transport due to a sudden stratospheric warming (e.g., Bailey et al., 2014). SOFIE  
236 sunset signals have lower signal correction errors, and the retrieved NO is reliable in more than  
237 half of the measurements below 80 km. SOFIE NO should not be used when PMCs are present  
238 due to the often extreme contamination, and these instances were filtered in the latest SOFIE V1.3  
239 NO product which is available online.

240 **Acknowledgements.** This work was funded by the AIM mission through NASA Small Explorer  
241 contract NAS5-03132. SOFIE data are available online at [sofie.gats-inc.com](http://sofie.gats-inc.com). ACE is funded by  
242 the Canadian Space Agency with P. Bernath (University of Waterloo and Old Dominion  
243 University) as the Mission Scientist. ACE data are available online at [database.scisat.ca](http://database.scisat.ca). MIPAS  
244 data are available online at [share.lsd.fkit.edu/imk/asf/sat/mipas-export/](http://share.lsd.fkit.edu/imk/asf/sat/mipas-export/).

## 245 **References**

- 246 Bailey, S. M., Thuraiajah, B., Randall, C. E., Holt, L., Siskind, D. E., Harvey, V. L.,  
247 Venkataramani, K., Hervig, M. E., Rong, P., and Russell, J. M. III: A multi tracer analysis of  
248 thermosphere to stratosphere descent triggered by the 2013 Stratospheric Sudden Warming,  
249 *Geophys. Res. Lett.*, 41, 5216–5222, doi:10.1002/2014GL059860, 2014.
- 250 Bender, S., Sinnhuber, M., von Clarmann, T., Stiller, G., Funke, B., López-Puertas, M., Urban, J.,  
251 Pérot, K., Walker, K. A., and Burrows, J. P.: Comparison of nitric oxide measurements in the  
252 mesosphere and lower thermosphere from ACE-FTS, MIPAS, SCIAMACHY, and SMR,  
253 *Atmos. Meas. Tech.*, 8, 4171-4195, <https://doi.org/10.5194/amt-8-4171-2015>, 2015.
- 254 Bermejo-Pantaleón, D., Funke, B., López-Puertas, M., García-Comas, M., Stiller, G. P., von  
255 Clarmann, T., Linden, A., Grabowski, U., Höpfner, M., Kiefer, M., Glatthor, N., Kellmann,



- 256 S., Lu, G.: Global observations of thermospheric temperature and nitric oxide from MIPAS  
257 spectra at 5.3  $\mu\text{m}$ , *J. Geophys. Res.*, 116, A10313, doi:10.1029/2011JA016752, 2011.
- 258 Bernath, P.: Atmospheric Chemistry Experiment (ACE): Mission Overview,  
259 Fourier Transform Spectroscopy/ Hyperspectral Imaging and Sounding of the Environment,  
260 24-27, doi:10.1364/FTS.2005.JMA3, 2005.
- 261 Funke, B., Stiller, G. P., Fischer, H., Glatthor, N., Grabowski, U., Hopfner, M.,  
262 Kellmann, S., Kiefer, M., Linden, A., Mengistu Tsidu, G., Milz, M., Steck, T., and Wang, D.  
263 Y.: Retrieval of stratospheric NO<sub>x</sub> from 5.3 and 6.2  $\mu\text{m}$  nonlocal thermodynamic equilibrium  
264 emissions measured by Michelson Interferometer for Passive Atmospheric Sounding  
265 (MIPAS) on Envisat, *J. Geophys. Res.*, 110, D09302, doi:10.1029/2004JD005225, 2005.
- 266 Garcia, R. R., Marsh, D. R., Kinnison, D. E., Boville, B. A., and Sassi, F.: Simulations of secular  
267 trends in the middle atmosphere, 1950–2003, *J. Geophys. Res.*, 112, D09301,  
268 doi:10.1029/2006JD007485, 2007.
- 269 Gomez-Ramirez, D., McNabb, J. W. C., Russell, J. M. III, Hervig, M. E., Deaver, L. E., Paxton,  
270 G., and Bernath, P. F.: Empirical correction of thermal responses in the SOFIE nitric oxide  
271 measurements and initial data validation results, *Appl. Optics*, 52, 2950–2959, 2013.
- 272 Gordley, L. L., Hervig, M., Fish, C., Russell, J. M. III, Bailey, S., Cook, J., Hansen, S., Shumway,  
273 A., Paxton, G., Deaver, L., Marshall, T., Burton, J., Magill, B., Brown, C., Thompson, E., and  
274 Kemp, J.: The Solar Occultation For Ice Experiment (SOFIE), *J. Atmos. Solar-Terr. Phys.*,  
275 71, 300-315, doi:10.1016/j.jastp.2008.07.012, 2009.
- 276 Hendrickx, K., Megner, L., Gumbel, J., Siskind, D. E., Orsolini, Y. J., Nesse Tyssøy, H., and  
277 Hervig, M.: Observation of 27 day solar cycles in the production and mesospheric descent of



278 EPP-produced NO, *J. Geophys. Res. Space Physics*, 120, 8978–8988,  
279 doi:10.1002/2015JA021441, 2015.

280 Hendrickx, K., Megner, L., Marsh, D., Gumbel, J., Strandberg, R., Martinsson, F.: Relative  
281 Importance of Nitric Oxide Physical Drivers in the Lower Thermosphere, *Geophys. Res.*  
282 *Letters*, 44, <https://doi.org/10.1002/2017GL074786>, 2017.

283 Hendrickx, K., Megner, L., Marsh, D. R., and Smith-Johnsen, C.: Production and transport  
284 mechanisms of NO in observations and models, *Atmos. Chem. Phys. Discuss.*, doi:  
285 10.5194/acp-2017-1188, 2018.

286 Hervig, M.E., Gordley, L.L., Stevens, M., Russell, J.M. III, Bailey, S., and Baumgarten, G.:  
287 Interpretation of SOFIE PMC measurements: Cloud identification and derivation of mass  
288 density, particle shape, and particle size, *J. Atmos. Solar-Terr. Phys.*, 71, 316-330,  
289 doi:10.1016/j.jastp.2008.07.009, 2009.

290 Kerzenmacher, T., Wolff, M. A., Strong, K., Dupuy, E., Walker, K. A., Amekudzi, L. K.,  
291 Batchelor, R. L., Bernath, P. F., Berthet, G., Blumenstock, T., Boone, C. D., Bramstedt, K.,  
292 Brogniez, C., Brohede, S., Burrows, J. P., Catoire, V., Dodion, J., Drummond, J. R., Dufour,  
293 D. G., Funke, B., Fussen, D., Goutail, F., Griffith, D. W. T., Haley, C. S., Hendrick, F.,  
294 Höpfner, M., Huret, N., Jones, N., Kar, J., Kramer, I., Llewellyn, E. J., López-Puertas, M.,  
295 Manney, G., McElroy, C. T., McLinden, C. A., Melo, S., Mikuteit, S., Murtagh, D., Nichitiu,  
296 F., Notholt, J., Nowlan, C., Piccolo, C., Pommereau, J.-P., Randall, C., Raspollini, P., Ridolfi,  
297 M., Richter, A., Schneider, M., Schrems, O., Silicani, M., Stiller, G. P., Taylor, J., Tétard, C.,  
298 Toohey, M., Vanhellemont, F., Warneke, T., Zawodny, J. M., and Zou, J.: Validation of  
299 NO<sub>2</sub> and NO from the Atmospheric Chemistry Experiment (ACE), *Atmos. Chem. Phys.*, 8,  
300 5801-5841, <https://doi.org/10.5194/acp-8-5801-2008>, 2008.



- 301 Newnham, D. A., Clilverd, M. A., Rodger, C. J., Hendrickx, K., Megner, L., Kavanagh, A. J.,  
302 Seppälä, A., Verronen, P. T., Andersson, M. E., Marsh, D. R., Kovács, T., Feng, W., Plane, J.  
303 M. C.: Observations and modeling of increased nitric oxide in the Antarctic polar middle  
304 atmosphere associated with geomagnetic storm-driven energetic electron precipitation. *J.*  
305 *Geophys. Res. Sp. Phys.*, 123, 6009–6025. [https://doi.org/ 10.1029/2018JA025507](https://doi.org/10.1029/2018JA025507), 2018.
- 306 Sheese, P. E., Walker, K. A., Boone, C. D., McLinden, C. A., Bernath, P. F., Bourassa, A. E.,  
307 Burrows, J. P., Degenstein, D. A., Funke, B., Fussen, D., Manney, G. L., McElroy, C. T.,  
308 Murtagh, D., Randall, C. E., Raspollini, P., Rozanov, A., Russell III, J. M., Suzuki, M.,  
309 Shiotani, M., Urban, J., von Clarmann, T., and Zawodny, J. M.: Validation of ACE-FTS  
310 version 3.5 NO<sub>y</sub> species profiles using correlative satellite measurements, *Atmos. Meas.*  
311 *Tech.*, 9, 5781-5810, <https://doi.org/10.5194/amt-9-5781-2016>, 2016.
- 312 Siskind, D. E., Sassi, F., Randall, C. E., Harvey, V. L., Hervig, M. E., Bailey, S. M., Russell, J. M.  
313 III: Is a high-altitude meteorological analysis necessary to simulate thermosphere-stratosphere  
314 coupling?, *Geophys. Res. Lett.*, 42, 8225–8230, doi:10.1002/2015GL065838, 2015.
- 315 Siskind, D. E., Jones Jr., M., Drob, D. P., McCormack, J. P., Hervig, M. E., Marsh, D. R.,  
316 Mlynczak, M. G., Bailey, S. M., Maute, A., and Mitchell, N. J.: On the relative roles of  
317 dynamics and chemistry governing the abundance and diurnal variation of low-latitude  
318 thermospheric nitric oxide, *Ann. Geophys.*, 37, 37-48, [https://doi.org/10.5194/angeo-37-37-](https://doi.org/10.5194/angeo-37-37-2019)  
319 2019, 2019.
- 320 Smith-Johnsen, C., Nesse Tyssøy, H., Hendrickx, K., Orsolini, Y., Kishore Kumar, G., Ødegaard,  
321 L.-K. G., Sandanger, M. I., Stordal, F., and Megner, L.: Direct and indirect electron  
322 precipitation effect on nitric oxide in the polar middle atmosphere, using a full-range energy



323 spectrum, *J. Geophys. Res. Space Physics*, 122, 8679–8693, doi:10.1002/2017JA024364,

324 2017.

325 Smith-Johnsen, C., Marsh, D. R., Orsolini, Y., Nesse Tyssøy, H., Hendrickx, K., Sandanger, M.

326 I., Glesnes Ødegaard, L., Stordal, F.: Nitric oxide response to the April 2010 electron

327 precipitation event: Using WACCM and WACCM-D with and without medium-energy

328 electrons. *J. Geophys. Res.: Space Physics*, 123, <https://doi.org/10.1029/2018JA025418>,

329 2018.

330